Comparative Study of the Photoprotolytic Reactions of D-Luciferin and Oxyluciferin

ARTICLE *in* THE JOURNAL OF PHYSICAL CHEMISTRY A · JUNE 2012

Impact Factor: 2.69 · DOI: 10.1021/jp301910p · Source: PubMed

THE JOURNAL OF PHYSICAL CHEMISTRY A

Article

pubs.acs.org/JPCA

Comparative Study of the Photoprotolytic Reactions of D-Luciferin and Oxyluciferin

Yuval Erez,[†] Itay Presiado,[†] Rinat Gepshtein,[†] Luís Pinto da Silva,[‡] Joaquim C. G. Esteves da Silva,[‡] and Dan Huppert*,[†]

[†]Raymond and Beverly Sackler Faculty of Exact Sciences, School of Chemistry, Tel Aviv University, Tel Aviv 69978, Israel

[‡]Centro de Investigação em Química, Departamento de Quimica, Faculdade de Ciencias da Universidade do Porto R. Campo Alegre 687, 4169-007 Porto, Portugal

Supporting Information

ABSTRACT: Optical steady-state and time-resolved spectroscopic methods were used to study the photoprotolytic reaction of oxyluciferin, the active bioluminescence chromophore of the firefly's luciferase-catalyzed reaction. We found that like D-luciferin, the substrate of the firefly bioluminescence reaction, oxyluciferin is a photoacid with pK_a* value of ∼0.5, whereas the excited-state proton transfer (ESPT) rate coefficient is 2.2×10^{10} s^{-1}, which is somewhat slower than that of D-luciferin. The kinetic isotope effect (KIE) on the fluorescence decay of oxyluciferin is 2.5 ± 0.1, the same value as that of D-luciferin. Both chromophores undergo fluorescence quenching in solutions with a pH value below 3.

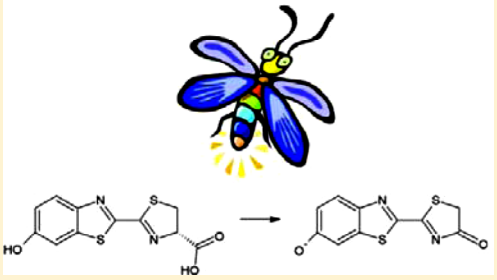

INTRODUCTION

Bioluminescence is a light-emitting phenomenon that occurs in living organisms, in which an excited-state product is formed in an enzyme-catalyzed reaction.[1−3] This enzyme is always termed luciferase, independently of the organism in which it is found.[4,5] The most studied bioluminescent system is that of the North American firefly, *Photinus pyralis*.[1−3,6] Firefly luciferase (Luc, EC 1.13.12.7) catalyzes a two-step reaction: first, the formation of an adenylyl intermediate (LH_2-AMP), by reaction of D-luciferin with adenosine-5′-triphosphate (ATP); second, the oxidation of LH_2-AMP. These latter reactions results in the formation of oxyluciferin in a singlet excited state.[1,6] The decay of the bioluminophore to the ground state is accompanied by emission of green light (∼562 nm, at basic pH).[2,7−9]

Oxyluciferin, shown in Scheme 1, is usually thought to exist in one of six chemical forms, by means of a quadruple chemical equilibrium (deprotonation of the two hydroxyl groups, and neutral and anionic keto−enol tautomerism of the thiazole ring).[10−13] However, due to the instability of this chromophore in basic solutions, little is known about its spectroscopic and structural properties. In fact, it was only recently that the identities of the species that emit in solution and in Luc active site were discovered. The work of Naumov et al. revealed that oxyluciferin exists in solution in its enol form, whereas theoretical studies have determined that the bioluminescence emitter is anionic keto-form oxyluciferin.[10,12,14,15]

Scheme 1. Oxyluciferin

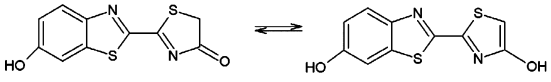

Previous studies have demonstrated that different factors can affect both the emission energy and the chemical equilibrium of oxyluciferin. Both experimental and theoretical studies have demonstrated that solvent polarity and various intermolecular interactions can modulate the emission wavelength of oxyluciferin, without the need of considering different species.[13,16−21] Also, several authors have demonstrated that the chemical equilibrium presented by oxyluciferin can be modulated by pH, solvent polarity and intermolecular interaction.[10−13,22]

Despite the difficulties of studying the spectroscopic properties of oxyluciferin, it was found that its absorption spectrum has a band at ∼420 nm for basic pH, and at ∼380 nm for acid-neutral pH.[10,22] The emission spectrum was found to be characterized by a peak at ∼550 nm.[10] Decreasing the polarity of the solvent leads to a blue-shift of both the absorption and emission maximum.

D-Luciferin (Scheme 2), besides being one of the substrates of the bioluminescence reaction, is one of the most useful analogues of oxyluciferin due to its similar spectroscopic properties and higher stability. The absorption spectrum of this molecule is characterized by a maximum at ∼330 nm in acidic solution and it is red-shifted at basic pH (∼390 nm).[23−30] The emission spectrum of D-luciferin has a maximum at ∼530 nm over the studied pH range 3−10. However, a decrease in the polarity of the solvent uncovers an emission band with a

Received: February 27, 2012
Revised: June 12, 2012
Published: June 14, 2012

Scheme 2. D-Luciferin

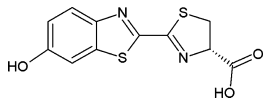

maximum at ~450 nm.[23−30] The red shift with increasing pH and polarity of the solvent is attributed to the deprotonation of the benzothiazole hydroxyl group.[23−30] In strongly acidic solutions an emission band at ~590 nm is found, which corresponds to the protonation of one of the nitrogen heteroatoms.[23−27]

In the current study we used time-integrated steady-state spectroscopy and time-resolved emission techniques to study the photoprotolytic reactions oxyluciferin undergoes. We then compared the obtained results with those of D-luciferin. We found that like D-luciferin, oxyluciferin is a photoacid, with a somewhat lower ESPT rate coefficient of 2.2×10^{10} s^{-1} (compared to 3.2×10^{10} s^{-1} of D-luciferin). Oxyluciferin, as does D-luciferin, undergo fluorescence quenching stemming either from geminate recombination with the proton or from excess protons in acidic media, where pH < 3.

EXPERIMENTAL SECTION

(4*S*)-2-(6-Hydroxybenzothiazole-2-yl)-4,5-dihydrothiazole-4-carboxylic acid (D-luciferin) 99.5% was purchased from Iris Biotech (Germany). HCl (1N) was purchased from Aldrich. Chemically synthesized oxyluciferin was obtained from 2-cyano-6-hydroxybenzothiazole and ethyl thioglycolate.[22,31] The parent compound 2-cyano-6-hydroxybenzothiazole was obtained from 2-cyano-6-methoxybenzothiazole (Aldrich, Steinheim, Germany).[22,31] For transient measurements the sample concentrations were between 2×10^{-4} and 2×10^{-5} M. Deionized water had a resistance of >10 MΩ. Methanol of analytical grade was purchased from Fluka. All chemicals were used without further purification.

The fluorescence up-conversion technique was employed in this study to measure the time-resolved emission of oxyluciferin at room temperature. The laser used for the fluorescence up-conversion was a cavity dumped Ti:Sapphire femtosecond laser, Mira, Coherent, which provides short, 150 fs, pulses at around 800 nm. The cavity dumper operated with a relatively low repetition rate of 800 kHz. The up-conversion system (FOG-100, CDP, Russia) operated at 800 kHz. The samples were excited by pulses of ~8 mW on average at the SHG frequency. The time response of the up-conversion system is evaluated by measuring the relatively strong Raman−Stokes line of water shifted by 3600 cm^{-1}. It was found that the fwhm of the signal is 300 fs. Samples were placed in a rotating optical cell to avoid degradation.

We used the time-correlated single-photon counting (TCSPC) technique to measure the time-resolved emission of oxyluciferin and D-luciferin. For sample excitations we used a cavity dumped Ti:Sapphire femtosecond laser, Mira, Coherent, which provides short, 80 fs, pulses. The TCSPC detection system is based on a Hamamatsu 3809U, photomultiplier and Edinburgh Instruments TCC 900 computer module for TCSPC. The overall instrumental response was about 40 ps (fwhm). The excitation pulse energy was reduced to about 10 pJ by neutral density filters.

SUMMARY OF PREVIOUS TIME-RESOLVED RESULTS OF D-LUCIFERIN

In previous papers we studied the photophysics and photochemistry of D-luciferin in water and water−methanol mixtures.[23−27] We found that D-luciferin is a photoacid. Photoacids are weak acids in their ground-state and much stronger acids in their first electronically excited state.[23−27,32−44] Usually, acidity is increased by more than seven pK_a units upon excitation. For a ground-state pK_a value of ~7, one expects an excited-state value of pK_a* ≤ 0. The rate of intermolecular ESPT to the solvent varies exponentially with the pK_a* value in the range 0.5−3. For pK_a* = 1, the expected rate coefficient is $\sim 5 \times 10^9$ s^{-1}, which is much higher than the radiative rate coefficient for an allowed transition, i.e., $k_r \sim 10^8$ s^{-1}. We found that D-luciferin is a strong photoacid with pK_a* of approximately 0, its ESPT rate coefficient is 3.2×10^{10} s^{-1}, and the kinetic isotope effect (KIE) on its fluorescence decay is ~2.5. The deprotonated form undergoes an effective fluorescence quenching by excess protons in aqueous solution. Scheme 3 describes the complex photoprotolytic reactions that

Scheme 3. Photoprotolytic Cycle of D-Luciferin and Oxyluciferin

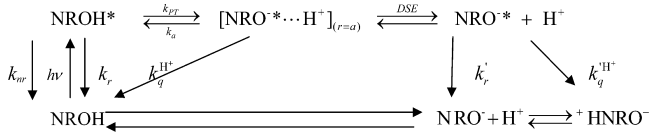

D-luciferin undergoes upon photoexcitation of the ground-state neutral protonated form, designated as NROH in the scheme. Upon excitation of the NROH form ESPT takes place to form the NRO^-*. The proton geminate recombination (reverse reaction) leads to ground-state NROH (k_q^{H+} in scheme 3). About half of the excited-state proton transfer events end up by fluorescence quenching whereas in the other events the proton is further removed from the NRO^-* molecules by a proton diffusion to the bulk (designated as DSE arrow in the scheme). The complexity of this reaction lies in the effective geminate recombination with the proton that leads to fluorescence quenching of the deprotonated form, NRO^-. There are two nitrogen atoms in the heterocyclic backbone of D-luciferin that can function as potential photobases. Upon excitation, these nitrogens may increase their basicity, so that they may snatch a proton from a nearby water molecule or react with a diffusing proton that was transferred to the solvent and form $^+HNRO^-$ that emits at 590 nm.

RESULTS

Steady State. Figure 1 shows the time-integrated steady-state excitation and emission spectra of oxyluciferin and D-luciferin in slightly acidic H_2O and D_2O solutions (pH ~ 6), respectively. The absorption maximum of the protonated NROH* form of D-luciferin and oxyluciferin are positioned at ~330 and 370 nm, respectively. The position of the NROH* emission band of both molecules is about the same (440 nm), whereas the position of the NRO^-* emission band of oxyluciferin (band maximum at 550 nm) is red-shifted with respect to that of D-luciferin by ~17 nm. The fluorescence intensity ratio $I^f_{NROH*}/I^f_{NRO^-*}$ is higher for oxyluciferin. This is an indication that D-luciferin is a stronger photoacid, provided that the radiative decay rates of both the NROH* and the

dx.doi.org/10.1021/jp301910p | J. Phys. Chem. A 2012, 116, 7452−7461

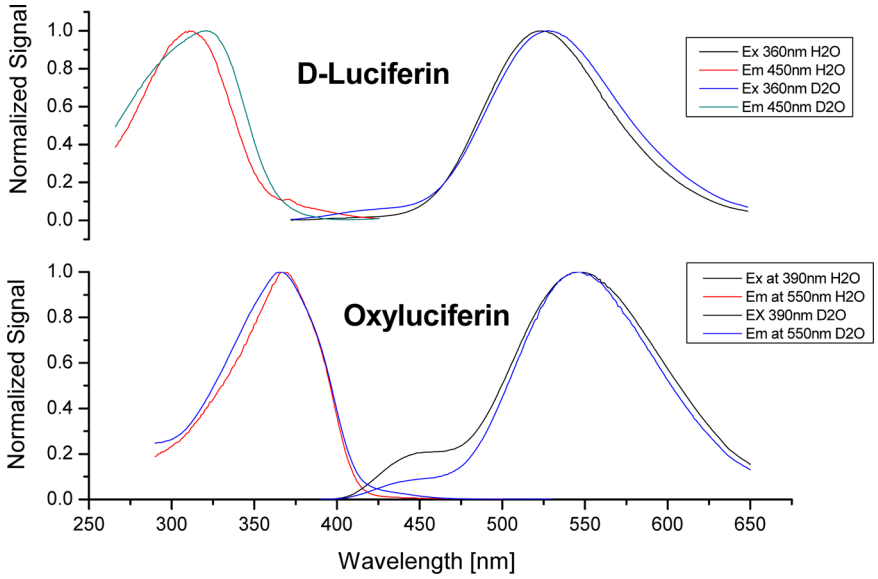

Figure 1. Time-integrated steady-state excitation and emission spectra in slightly acidic H_2O and D_2O solution (pH ~ 6), respectively, of (a) oxyluciferin and (b) D-luciferin.

NRO^-* forms of both D-luciferin and oxyluciferin are the same. The reality, however, is more complex, as will be shown by the time-resolved measurements. The absorption spectra of oxyluciferin in H_2O at several pH values are given in Figure s1d in the Supporting Information. At pH = 5 the absorption spectrum in the spectral range of 330−500 nm consists of two bands with peaks at 370 and 420 nm, which overlap to a great extent. At lower pH the intensity of the 420 nm band decreases, whereas that of the ~370 nm band increases. Two isosbestic points, at ~397 and 324 nm, are clearly seen. When the sample is excited at 374 nm, the emission spectrum consists of two bands; a weak band at 440 nm and a stronger one at 550 nm. Upon excitation at 420 nm, there is only a single band at ~550 nm, which is similar to the 550 nm band appearing when samples are excited in acidic solution at 370 nm.

Time-Resolved Emission. *Time-Correlated-Single-Photon-Counting Measurements.* Figures 2 and s1a in the Supporting Information show on linear and semilogarithmic scales the time-resolved emission of oxyluciferin in water at several wavelengths measured by the TCSPC technique, which is a highly sensitive method with a good signal-to-noise ratio and a wide dynamic range. The time resolution of this technique, however, is limited to ~20 ps and the full width half-maximum of the instrument's response function (IRF) is ~40 ps.

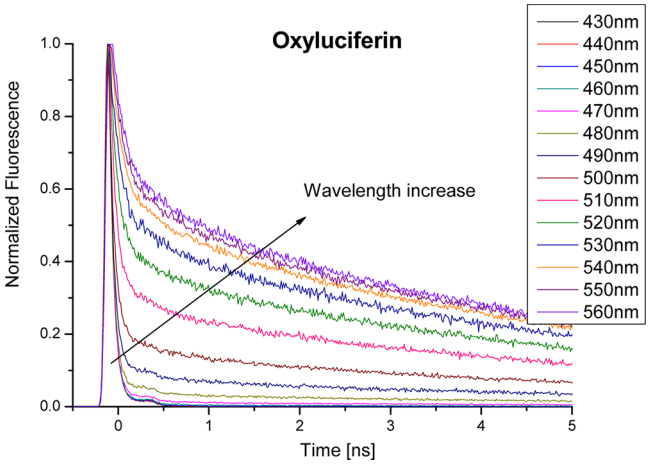

Figure 2. TCSPC time-resolved emission of oxyluciferin in water at several wavelengths.

As seen in the figures, the protonated NROH* form's signals measured at $\lambda \leq 470$ nm decay fast, whereas the signals at $\lambda \geq 510$ nm, mainly attributed to the NRO^-* species, have a bimodal decay curve with a short and long time decay components. Parts b and c of Figure s1 (Supporting Information) show biexponential fits of the fluorescence signals shown in Figures 2 and s1a (Supporting Information). The parameters of these fittings are given in Table s1 (Supporting Information).

Kinetic Isotope Effect. Figures 3 and s2 (Supporting Information) show on linear and semilogarithmic scales the time-resolved emission of oxyluciferin in both H_2O and D_2O, where in each panel the two signals are compared at a selected wavelength. The decay rate of the main fluorescence decay component at $\lambda \leq 470$ nm attributed to the protonated form is fast, and it is slower in D_2O than in H_2O. We therefore assign this fast decay component to ESPT to the solvent. In previous studies on ESPT processes of photoacids, we found that the kinetic isotope effect (KIE) is around 3 for photoacids with $pK_a^* > 0.4$, and this value reduces the stronger the photoacid. For D-luciferin we found that the KIE = 2.5 ± 0.1. Using a multistretched exponential decay function to fit the data, we found that the short-time decay component of oxyluciferin is 47 ± 5 ps and 118 ± 10 ps in H_2O and D_2O, respectively. The KIE value for oxyluciferin is therefore 2.5 ± 0.2, a figure that closely resembles that of D-luciferin. The values of the fitting parameters of the time-resolved emission of the signals for oxyluciferin in H_2O and D_2O at several wavelengths are given in Tables s1 and s2 (Supporting Information), respectively. Tables s3 and s4 (Supporting Information) provide the fitting parameters for D-luciferin in H_2O and D_2O, respectively. Detailed description of the fitting procedure is given in the Supporting Information.

The oxyluciferin signals at $\lambda \leq 500$ nm could be reasonably fitted by a large component (≥0.9) with a lifetime of 47 and

dx.doi.org/10.1021/jp301910p | J. Phys. Chem. A 2012, 116, 7452−7461

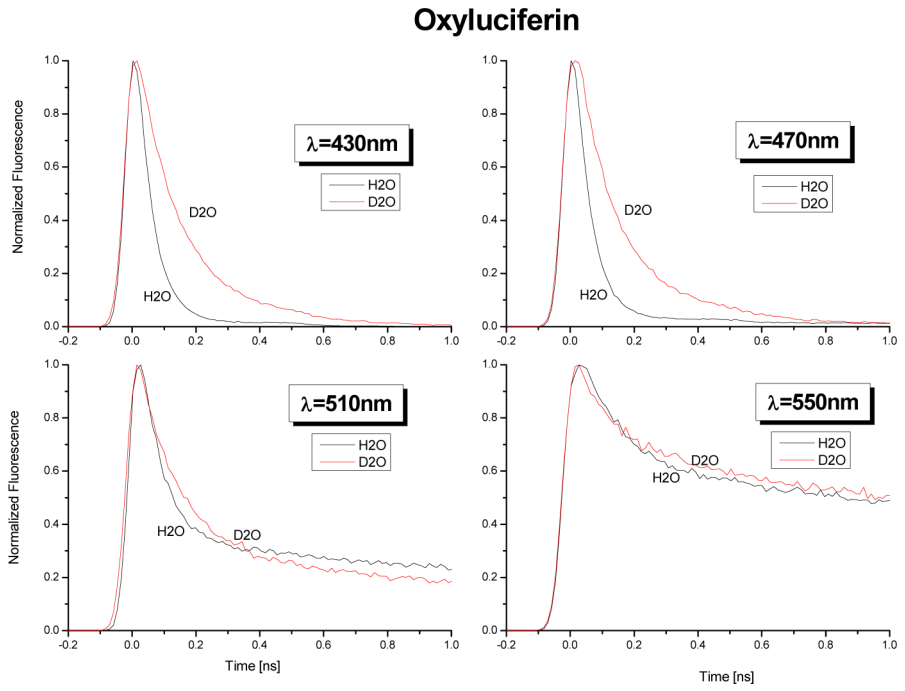

Figure 3. Time-resolved emission of oxyluciferin in both H_2O and D_2O.

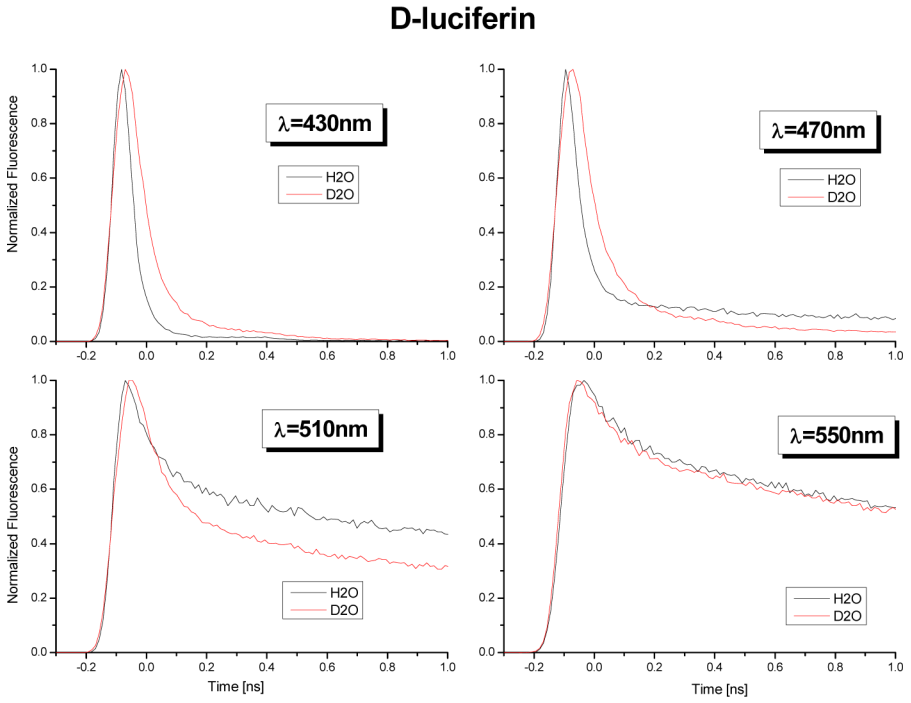

Figure 4. Time-resolved emission of D-luciferin in both H_2O and D_2O at pH ~ 6, excited by 150 fs pulses at 385 nm.

118 ps in H_2O (Table s1, Supporting Information) and D_2O (Table s2, Supporting Information) respectively. A long-time minor component (<0.1) of 5.2 ns in H_2O and 8.2 in D_2O is present in all the short wavelength measurements. At 460 nm, the amplitude of the long-time decay component is only 0.003. However, as the monitored wavelength becomes longer, the amplitude of this component also increases. Similar parameters were found for the fit of the D-luciferin signals. At $\lambda \geq 510$ nm the oxyluciferin signals have a relatively fast decay component of 0.13 ns in H_2O and 0.18 ns in D_2O with an amplitude of about 0.5 at 540 nm, followed by a long component, of 3.8 and 4.6 ns in H_2O and D_2O respectively. We attribute the short component at long wavelengths, $\lambda \geq 510$ nm to the irreversible recombination of the nitrogen atoms of the thiazole rings with the proton. The long lifetime is due to the radiative decay process of oxyluciferin in these solvents.

Figures 4 and s3 show on linear and semilogarithmic scales the time-resolved emission of D-luciferin in both H_2O and D_2O at pH ~ 6, excited by 150 fs pulses at 385 nm. In each panel the two signals are compared at a given wavelength, in much the same way as the signals of oxyluciferin are given in Figure 3. At $\lambda \leq 470$ nm the signal's decay curve mainly consists of a short-

dx.doi.org/10.1021/jp301910p | J. Phys. Chem. A 2012, 116, 7452−7461

time component, which exhibits a distinctive KIE. The decay time of the short component is 30 ± 5 ps in H_2O and 75 ± 10 ps in D_2O. We reported similar results in a previous article.[23] The decay times of D-luciferin in both H_2O and D_2O are 1.6 times shorter than those of oxyluciferin. At $\lambda \geq 510$ nm the fluorescence decay is bimodal, much like oxyluciferin. It has a short time decay component of ∼100 ps and a relative amplitude of 0.5 at $\lambda \geq 530$ nm, which is the peak of the NRO^-* band. As in the case of oxyluciferin, the time constant of the long-time component of the fluorescence decay of the NRO^-* band varies with the solvent, $\tau_{H_2O} \simeq 3.9$ ns and $\tau_{D_2O} \simeq 4.6$ ns. The KIE is therefore 1.18, a considerably lower value than that of oxyluciferin (1.6). The lifetime of the NRO^-* form in both H_2O and D_2O is shorter than in oxyluciferin.

Parts a and b of Figure s4 (Supporting Information) show on linear and semilogarithmic scales the time-resolved emission signals of both D-luciferin and oxyluciferin in D_2O. In each panel the two signals are shown in a given wavelength. At $\lambda \leq$ 470 nm the fluorescence decay of the ROH* of D-luciferin is much shorter than that of oxyluciferin. At 550 nm the decay times of the short components of both molecules have roughly the same value around 100 ps, whereas the time constant of the long component is 8.2 and 4.6 ns for oxyluciferin and D-luciferin, respectively.

To summarize this subsection, the D-luciferin ESPT rate constant in water, $k_{PT} = 3.2 \times 10^{10}$ s^{-1} is somewhat larger than that of oxyluciferin $k_{PT} = 2.2 \times 10^{10}$ s^{-1}. Both compounds have the same KIE of 2.5 when the solvent is replaced by D_2O. The emission of the NRO^- deprotonated form has a lifetime of 3.8 ns for D-luciferin and 5.2 ns for oxyluciferin. Both D-luciferin's and oxyluciferin's NRO^- time-resolved emission is bimodal with a short component decay time of about 130 ps and an amplitude of about 0.35.

Up-Conversion Fluorescence Measurements. Figures 5 and s5 show the fluorescence up-conversion signals of oxyluciferin

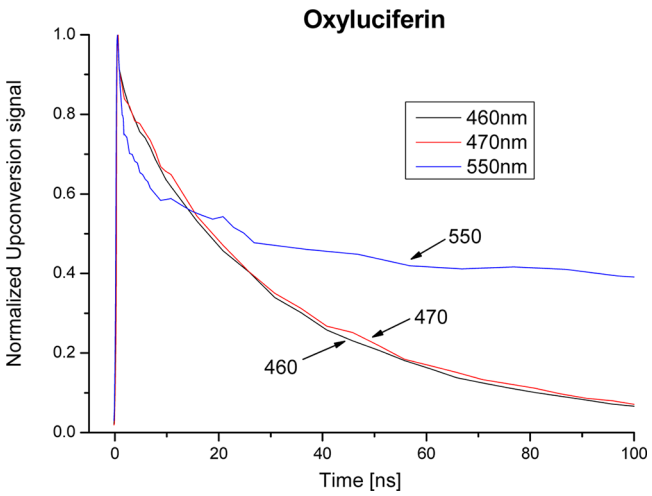

Figure 5. Fluorescence up-conversion signals of oxyluciferin at several wavelengths.

at several wavelengths. The time resolution of the up-conversion technique is approximately 100 times better than that of the TCSPC technique. The full width half-maximum of the IRF is ∼300 fs compared with ∼45 ps of the TCSPC. The up-conversion technique is about 3 orders of magnitude less sensitive than TCSPC, and consequently, the signal-to-noise ratio and the dynamic range are also smaller than TCSPC.

The signals have a short component of a few picoseconds followed by a longer nonexponential component. The average decay time of the long component is ∼45 ps, which is comparable to the value obtained from the TCSPC signal of 47 ps, attributed to the ESPT rate to the solvent. The up-conversion signal measured at 550 nm does not have a rise component, as expected due to the NRO^-* creation reaction, i.e., NROH* → NRO^-* + H^+. The TCSPC signals measured at $\lambda \geq 530$ nm, and whose time resolution is much lower, also do not have a rise component. We suggest that this is due to an efficient nonradiative process, assisted by protons first transferred to the solvent and then recombined with the NRO^-* on the nitrogen site via a solvent bridge. The nitrogen atom is a mild base in the electronic ground state of heterocyclic compounds, and a much stronger base in the excited state. We therefore suggest that the nonexponential decay curve of the NRO^-* is due to an excited-state recombination process with the proton, NRO^-* + H^+ → NROH(g). A similar finding was reported and a similar explanation was offered previously in our study on the photophysics and photochemistry of D-luciferin.[23]

Figure 6a shows the fluorescence up-conversion signals of D-luciferin in water measured at several wavelengths. As seen in the figure, the average decay times of the D-luciferin signals are shorter than those of oxyluciferin. Figure 6b shows the oxyluciferin and D-luciferin signals measured at 470 nm. As seen in this figure, the oxyluciferin signal's decay time is longer than that of D-luciferin. At $\lambda \geq 530$ nm, the fluorescence up-conversion signal of D-luciferin (shown in Figure 6a) has a distinct rise component, whereas the oxyluciferin signal at long wavelengths does not (Figure 5). We consider the cause of this difference to be the faster proton-assisted quenching rate of oxyluciferin.

Time-Resolved Spectra of Oxyluciferin and D-Luciferin. Figure 7 shows the constructed normalized time-resolved emission spectra of oxyluciferin and D-luciferin in H_2O at several times in the range 50 fs to 1 ns. We constructed the spectra as follows. We assumed that at 2 ps the spectrum mainly consists of the NROH* emission and a smaller contribution from the NRO^-*. The shapes of the NROH* and NRO^-* emission bands at 2 ps are assumed to be roughly the same as those measured with the steady-state fluorometer. This assumption somewhat distorts the constructed spectra because it does not fully account for spectral shifts associated with solvation dynamics. Fortunately, the spectral shifts in the case of both chromophores are relatively small. This is shown in Figure 2, where the time-resolved fluorescence signals of the oxyluciferin NROH* band (430−470 nm) are nearly identical. When the change in solvent reorganization energy is low, the time-dependent band shift is small and the approximation is justified. The spectra shown in the figure were constructed from the time-resolved emission signals of the chromophores in water, and sampled in 10 nm intervals in the spectral range 430−560 nm. As seen in the figure, the NROH* band intensity diminishes with time. The time-resolved spectra of both chromophores have similar time dependence and spectral behavior. The intensity of the NROH* band decreases over time, whereas that of the NRO^-* band increases. The rates at which the NROH* decreases and the NRO^-* increases are similar. We therefore conclude that oxyluciferin and D-luciferin undergo ESPT to the solvent. Figures s6−s8 (Supporting

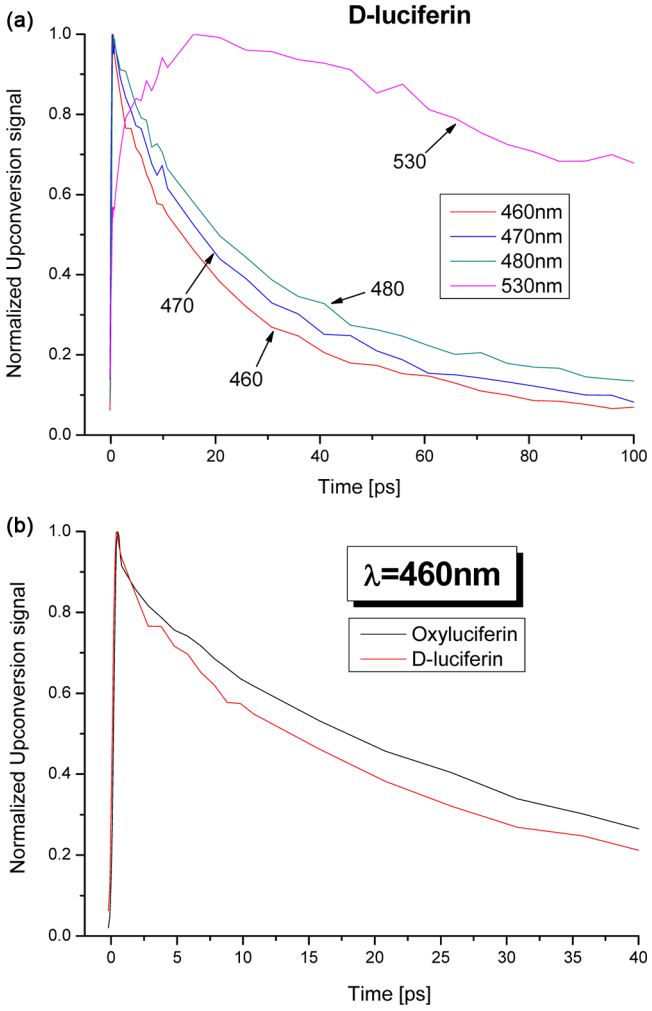

Figure 6. (a) Fluorescence up-conversion signals of D-luciferin in water measured at several wavelengths. (b) Fluorescence up-conversion signals of oxyluciferin and D-luciferin in water measured at 460 nm.

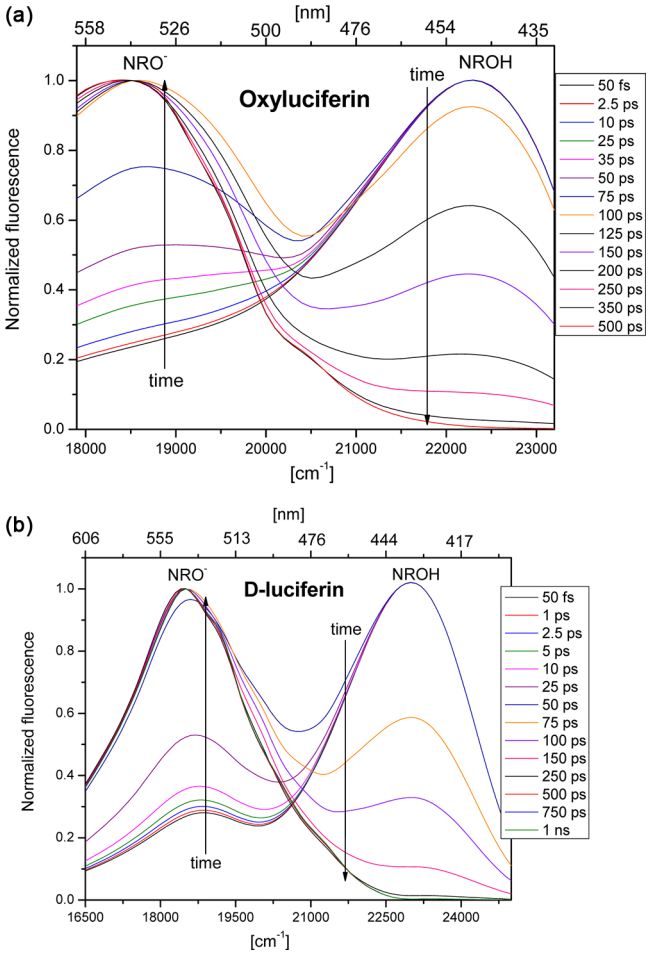

Figure 7. Normalized time-resolved emission spectra constructed from TCSPC signals: (a) oxyluciferin in H_2O; (b) D-luciferin in H_2O.

Information) show the time-resolved spectra of D-luciferin in H_2O and of oxyluciferin in both H_2O and D_2O. As expected, the rate of ESPT in D_2O is slower by a factor of 2.5 than in H_2O. A good criterion to the fit quality is the constructed steady-state spectra by time integration of the time-resolved spectra. This is shown in Figures s6c, s7c, and s8c in the Supporting Information. The figures show the steady-state emission spectra of oxyluciferin and D-luciferin in H_2O and also oxyluciferin in D_2O measured by a fluorometer against the constructed steady state by time integration of the time-resolved spectra. As seen in the figures, the constructed steady state qualitatively fits the measured spectra. We are unable to identify a new band that can be assigned to the keto/enol equilibrium that may take place on the thiazole ring.

Acid Effect. Figure 8 shows the time-resolved TCSPC emission signals of the NROH* of oxyluciferin at 440 nm and the NRO^{-}* at 540 nm in several acidic aqueous solutions. The NROH* signals are almost invariant under change of the acid concentration (Figure 8a), whereas the decay of NRO^{-}* signals varies with the concentration of the acid such that the higher its concentration the faster the decay rate. A similar acid effect was previously observed for D-luciferin. The excess protons in the solution react with the NRO^{-}* to form NROH(g). This reaction is diffusion-controlled, where the proton diffusion constant, $D_{H^+} \approx 10^{-4}$ cm^2/s, and the diffusion-controlled reaction rate coefficient, $k_D = 5 \times 10^{10}$ M^{-1} s^{-1}, for a reaction between the proton cation and the NRO^{-}* species anion. Thus, an acid concentration of 10 mM reduces the long decay time component of the NRO^{-}* from 5.2 ns to ~2 ns.

To summarize the acid effect, for both D-luciferin and oxyluciferin the main fluorescence band assigned to the NRO^{-} form is quenched when acid is added to aqueous solution, the quenching rate is diffusion controlled.

Methanol–Water Mixtures. Figure 9 shows the time-resolved emission of the NROH* (440 nm) and NRO^{-}* (540 nm) forms of oxyluciferin in several water–methanol mixtures. The signals of the NROH* are strongly dependent on the methanol concentration. In almost pure methanol (~99%) the decay time is rather long, i.e., 1.6 ns, whereas in a mixture of 95% water (by volume) the decay time is 47 ps. Similar dependence on the water–methanol mixture's composition is shared by many photoacids. For strong and weak photoacids whose $pK_a^* \geq 0$ the ESPT rate in methanol is 100 times slower than in water. Thus, an ESPT process with a time constant of 50 ps in water is expected to take 5 ns in methanol, which is about the same as the radiative lifetime of an allowed transition from a ground-state singlet state to an excited singlet state. According to the Marcus model, which relates the rate coefficient of a reaction and its free energy, the rate coefficient of reactions where $\Delta G > 0$ scales approximately exponentially

dx.doi.org/10.1021/jp301910p | J. Phys. Chem. A 2012, 116, 7452–7461

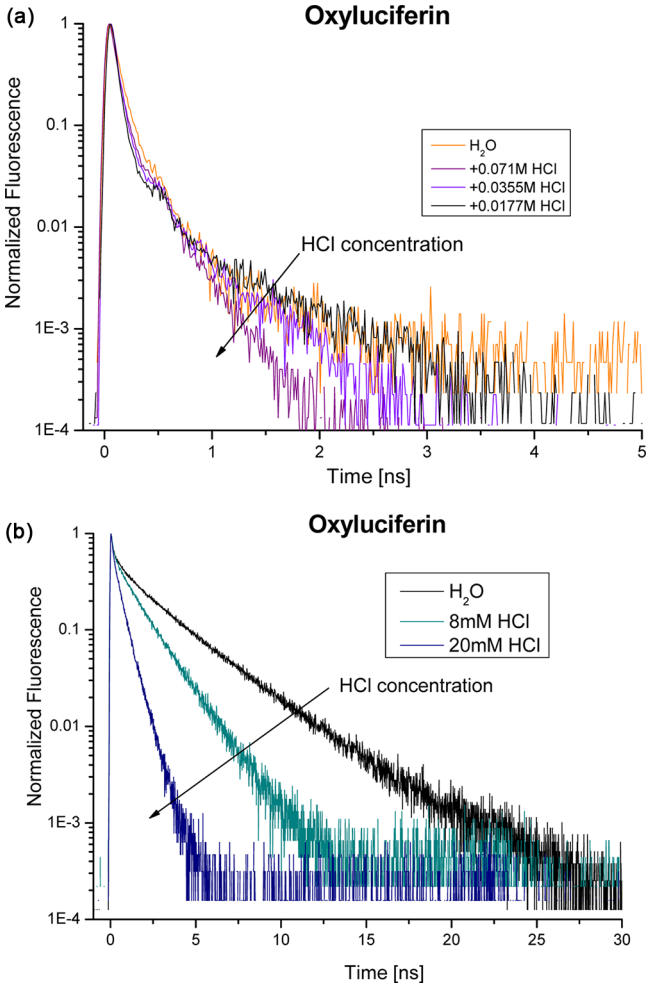

Figure 8. Time-resolved TCSPC emission signals of oxyluciferin in several acidic aqueous solutions measured at (a) 440 nm and (b) 540 nm.

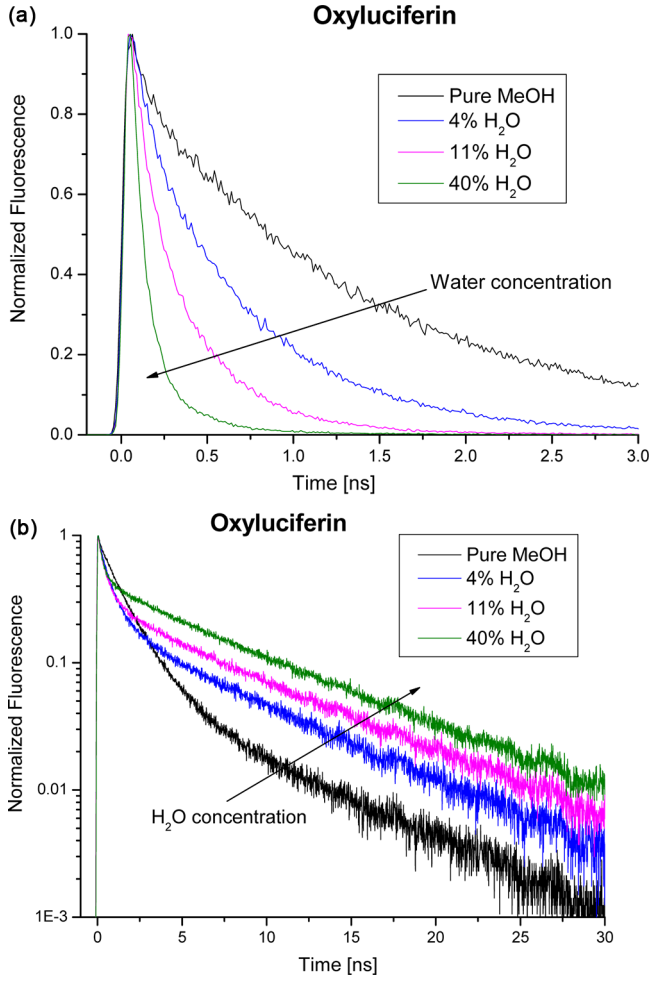

Figure 9. Time-resolved emission of oxyluciferin in several water–methanol mixtures: (a) NROH* (440 nm) form; (b) NRO^{-}* (540 nm) forms.

with the pK_a* value. For a weak photoacid with pK_a* value of ~1.5, the ESPT rate coefficient in water is ~10^9 s^{-1}. In these instances the radiative rate is much faster than the ESPT rate in methanol (10^7 s^{-1}), and thus the efficiency of the ESPT process is very low. The steady-state fluorescence spectrum of weak photoacids in methanol exhibits mainly the emission band of the protonated form and only ~1% of the deprotonated form, whereas in water both the protonated and deprotonated forms' emission bands appear.

The TCSPC signals shown in Figure 9b are bimodal and can be fitted by short and long decay components. The amplitude of the short decay component in water–methanol mixtures decreases as the water concentration increases. The decay time is independent of the mixture's composition. The lifetime of the long-time decay component is almost independent of the mixture's composition, as its value in neat water and neat methanol (and every volumetric ratio in between) is nearly the same. In neat methanol the amplitude of the short time decay component of the TCSPC signal at 540 nm is ~0.98. We attribute the short-time component of the 540 nm signal to the NROH* emission, whereas the long-time decay component, whose amplitude is 0.02, to the NRO^{-}* band. The 1.6 ns decay of the signal at 440 nm is similar to the decay time of the major component of the 540 nm signal.

Figure s9 in theSupporting Information shows the steady-state emission spectrum and the excitation of oxyluciferin in methanol. The emission spectrum consists of only the NROH band with a band maximum at ~445 nm. For D-luciferin, we found that it is capable in the excited state to transfer a proton in neat methanol and thus the steady-state spectrum consists of a strong NROH band and a weak NRO^{-} band.[24]

The emission spectrum of oxyluciferin in methanol consists of only the NROH* band, whereas in water the emission bands of both forms appear in the spectrum upon excitation of the ground-state NROH (Figure 1). Similar dependence of the time-resolved emission on the water–methanol mixture's composition was previously reported in our study on D-luciferin. The decay time of the NROH* band decreases the more aqueous the mixture becomes. However, even in pure methanol two bands appear in the D-luciferin emission spectrum, and the decay time of the NROH* is ~400 ps, indicating that ESPT does indeed take place. We therefore conclude that between these two homologous molecules D-luciferin is the stronger photoacid. This conclusion is also backed by the larger ESPT rate coefficient of D-luciferin in water of 3.3 × 10^{10} s^{-1} compared to 2.1 × 10^{10} s^{-1} of oxyluciferin.

Basic Solution. Figure 10 shows the steady-state excitation and emission spectra of oxyluciferin and D-luciferin in aqueous

dx.doi.org/10.1021/jp301910p | J. Phys. Chem. A 2012, 116, 7452–7461

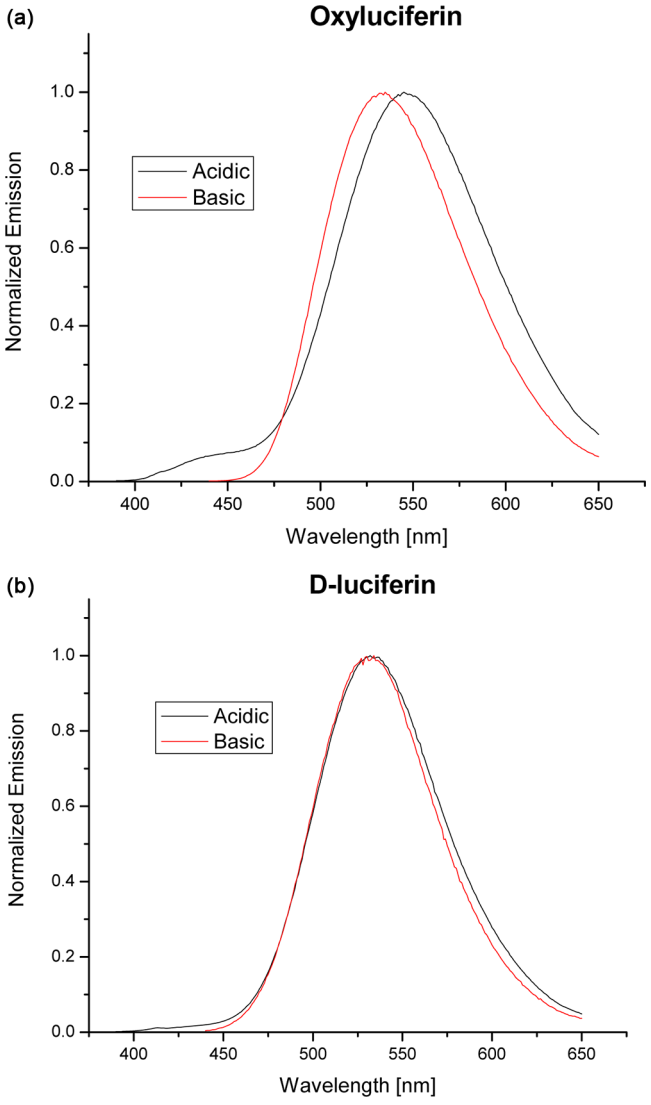

Figure 10. Steady-state excitation and emission spectra in aqueous acidic (pH ~ 4.5) and basic (pH ~ 9) solutions of (a) oxyluciferin and (b) D-luciferin.

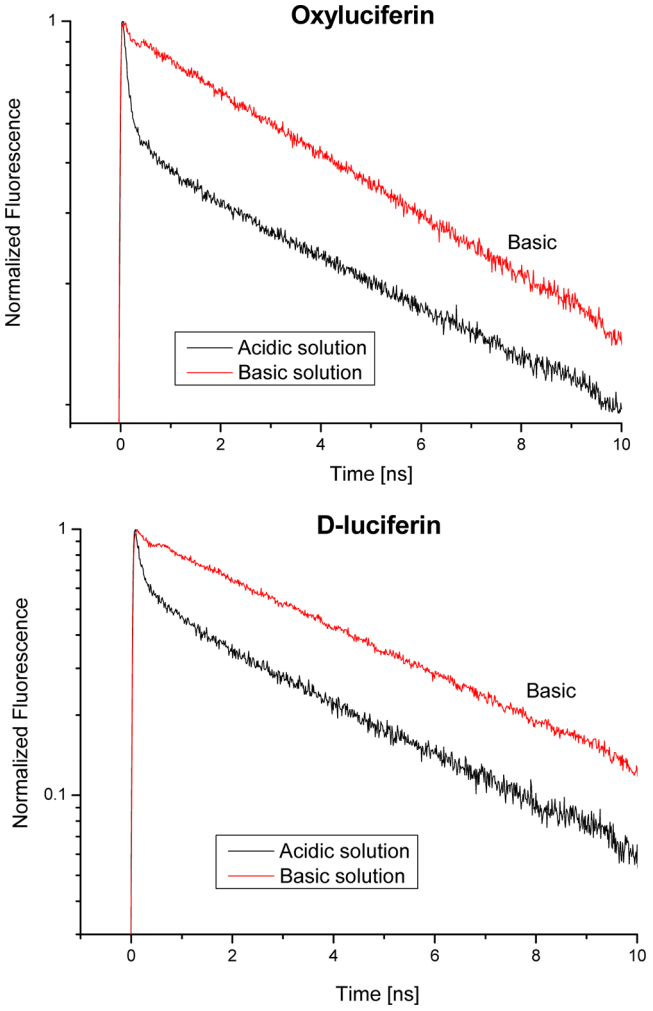

Figure 11. Time-resolved emission of the deprotonated NRO^{-}* form in both acidic (pH ~ 4.5) and basic (pH ~ 9) aqueous solutions of (a) oxiluciferin and (b) D-luciferin.

acidic (pH ~ 4.5) and basic (pH ~ 9) solutions, respectively. The oxyluciferin and D-luciferin spectra in the acidic solutions, where the molecules were excited at their NROH form's absorption band, are composed of two bands: a weak NROH* band and a strong NRO^{-}* band. The position of the peak of the NRO^{-}* band of oxyluciferin in basic solution is at ~540 nm, whereas its peak position upon excitation of the NROH form is at ~550 nm. The emissions of the NRO^{-}* of D-luciferin in both basic and acidic solutions are almost identical in their shapes and positions. We are unaware of previous reports on large changes in the position of the emission band of oxyluciferin as a function of the pH value of the solution. We are not yet certain of the origin of this strong pH effect on the NRO^{-}* band's position, though we suspect it is related to the tautomerization of the thiazole ring (Scheme 2) or to a second ionization of the excited-state species.[12]

Figure 11 shows the time-resolved emission of the deprotonated NRO^{-}* form of oxyluciferin and D-luciferin in both acidic and basic aqueous solutions, respectively. The TCSPC NRO^{-}* signals (measured at the peak of the emission band) of both oxyluciferin and D-luciferin in acidic solutions consist of a fast decaying component and a slow one. In basic solution the amplitude of the short component of the NRO^{-}* signal of both D-luciferin and oxyluciferin is smaller than 0.05, whereas in acidic solution its value is ~0.35. As aforesaid, we attribute the short component to fluorescence quenching by the geminate recombination with the proton probably occurring at one of the nitrogen atoms. In basic solutions, recombination does not occur because a proton is not transferred to the solution to begin with.

a. **Main Findings.** The ground-state pK_a measured for a 30% methanol in water rich methanol mixtures by absorption is ~7.
b. The steady-state emission measurements clearly show that when the NROH form is excited the spectrum consists of a dual emission band. The bands are assigned to the NROH* and NRO^{-}* forms.
c. The decay time of the time-resolved emission signal of the NROH* form is ~45 ps in H_2O and ~120 ps in D_2O.
d. The TCSPC signals of the NRO^{-}* measured at long wavelengths are bimodal with a short time decay component, whose average lifetime is about 0.2 ns, and a long decay time of about 5.2 and 8.2 ns in H_2O and D_2O, respectively, for the long component.

dx.doi.org/10.1021/jp301910p | J. Phys. Chem. A 2012, 116, 7452−7461

e. In acidic aqueous solutions the time-resolved TCSPC emission signals of the NROH* form are only slightly affected at an acid concentration of up to 20 mM, whereas the decay time of the long component of the NRO^-* decay decreases linearly with the acid concentration. The strong acid effect on the NRO^-* emission lifetime is attributed to recombination with the proton that leads to a ground-state NROH (g).

f. The ESPT rate of photoacids with $pK_a^* \geq 0.5$ in methanol is slower than in water by a factor of 100 or more. This is also true for oxyluciferin, a mild photoacid that is incapable of transferring a proton to methanol. D-Luciferin, however, is a stronger photoacid that can also transfer a proton to methanol.

DISCUSSION

The experimental results clearly show that like D-luciferin, oxyluciferin is a photoacid. In the ground state it is a weak acid with pK_a value of ~7, whereas in the electronically excited state it becomes a much stronger acid. We estimate the pK_a^* value to be approximately 0.5, which is roughly the pK_a^* of 2N68DS.

The ESPT rate coefficient of oxyluciferin in H_2O is 2.2×10^{10} s^{-1}, which is slightly lower than that of D-luciferin, i.e., 3.2×10^{10} s^{-1}.

The molecular backbone of both compounds is very similar. The difference lies in that the D-luciferin thiazole moiety is bonded to a carboxylic group, whereas the same moiety in oxyluciferin can present a ketonic or enolic functional group (Schemes 1 and 2). The pK_a^* values of 2N, its sulfonate derivatives, and cyano derivatives are smaller by about 7 orders of magnitude than their pKa values. 2N has a pK_a^* value of ~2.7 and that of 2N68DS is 0.5, whereas cyanonaphthols are even stronger with negative pK_a^* values, e.g., 5,8-dicyano-2-naphthol whose pK_a^* value is ~−4. Calculations have shown that the main indication to a photoacid's strength is the excited-state energy of the deprotonated form with respect to that of the protonated form. The more electron withdrawing functional groups bonded to the aromatic rings there are, the lower the energy of the deprotonated form and the stronger the photoacid, thus delocalizing the effective charge of the hydroxylate group and the overall energy of the deprotonated form.

D-Luciferin and oxyluciferin are different from other photoacids, because there is a large fluorescence quenching of the deprotonated NRO^-* form, when the molecule is excited from the ground-state NROH form, and the NRO^-* is the product of the photoprotolytic process (Scheme 3).

In general, photoacids can be divided into two groups, reversible and irreversible photoacids. For reversible photoacids, the second step in the photoprotolytic process, after a forward reaction, in which a proton is transferred to the solvent, is a diffusion-assisted geminate recombination of the deprotonated form with the proton to reform the excited protonated form of the photoacid. Irreversible photoacids, which undergo geminate recombination, however, decay to the ground state and therefore the fluorescence of the deprotonated form of an irreversible photoacid is weaker than that of a reversible one. In acidic solution (pH ≤ 3) the steady-state emission band intensity of the deprotonated form decreases linearly with the acid concentration. The time-resolved fluorescence decay curve on a semilogarithmic scale, of a deprotonated form of an irreversible photoacid is concave in solutions where the pH level is in the range 4−7. The concave shape is explained by the diffusion-assisted irreversible geminate recombination reaction with the proton. The amplitude of the fast component, seen in the NRO^- fluorescence decay of both D-luciferin and oxyluciferin is much larger than expected from a regular irreversible photoacid such as 1-naphthol and its sulfonate derivatives. The amplitude of the fast component in the emission of the RO^-* of 1N4S for example, is much smaller than those of both luciferin compounds. We therefore attribute this fast quenching process of the luciferins to the irreversible geminate recombination of the proton with the nitrogen of the thiazole ring, leading to an efficient fluorescence quenching. This reaction is efficient because it is probably assisted by a water bridge forming a proton wire between the hydroxyl group and the nitrogen.

SUMMARY

Oxyluciferin is the active chromophore of the bioluminescence luciferase enzyme-catalyzed reaction taking place in fireflies, for which D-luciferin acts as a substrate. These two compounds (shown in Schemes 1 and 2) are photoacids. The photoacidic functional group is the hydroxyl at position six on the 6-hydroxybenzothiazole moiety. On the thiazole, D-luciferin has a carboxylic group where oxyluciferin is in either a ketone or enol form. In the current study, we compare the photophysical and photochemical properties of both compounds. For this purpose, both time-resolved TCSPC and fluorescence up-conversion techniques were used. Both compounds are weak acids in their electronic ground state with a pK_a value of ~7. In the excited state, the acidity of both molecules increases by more than seven pK_a units. The rate coefficient of the ESPT to the solvent is high, i.e., 3.3×10^{10} and 2.1×10^{10} s^{-1} for D-luciferin and oxyluciferin, respectively. There is a strong KIE on both molecules' fluorescence decays of 2.5 ± 0.1. Fluorescence of both molecules' NRO^-* form is unusually quenched when excited from their NROH form (Scheme 3). The fluorescence decay of the NRO^-* form is bimodal with a minor component of 100 ps and an amplitude of 0.35 followed by a major component of 3.8 and 5.2 ns for D-luciferin and oxyluciferin, respectively. The fluorescence decay of the NRO^-* form of both compounds, when the molecules are in a basic solution and excited from their NRO^- form, is nearly exponential. We attribute the fast fluorescence quenching rate to the geminate recombination of the proton with NRO^-* at a nitrogen atom site that leads to the formation of the ground-state zwitterion $^+HNRO^-$.

ASSOCIATED CONTENT

Supporting Information

Time-resolved TCSPC and fluorescence up-conversion emission figures on semilogarithmic scale. Data fitting procedure and tables of fitting parameters. Time-resolved spectra of oxyluciferin in H_2O, D_2O, and methanol. This information is available free of charge via the Internet at http://pubs.acs.org

AUTHOR INFORMATION

Corresponding Author

*E-mail: huppert@tulip.tau.ac.il. Tel: 972-3-6407012. Fax: 972-3-6407491.

Notes

The authors declare no competing financial interest.

■ ACKNOWLEDGMENTS

This work was supported by grants from the Israel Science Foundation and from the James-Franck German-Israeli Program in Laser-Matter Interaction. Financial support from Fundação para a Ciência e Tecnologia (FCT, Lisbon) (Programa Operacional Temático Factores de Competitividade (COMPETE) e comparticipado pelo Fundo Comunitário Europeu (FEDER) (Project PTDC/QUI/71366/2006) is acknowledged. A Ph.D. grant to Luís Pinto da Silva (SFRH \76612\2011), attributed by FCT, is also acknowledged.

■ REFERENCES

(1) Marques, S. M.; Esteves da Silva, J. C. G. *IUBMB Life* **2009**, *61*, 6−17.
(2) Pinto da Silva, L.; Esteves da Silva, J. C. G. *J. Chem. Theory Comput.* **2011**, *7*, 809−817.
(3) Leitão, J. M.; Esteves da Silva, J. C. G. *J. Photochem. Photobiol. B* **2010**, *101*, 1−8.
(4) Viviani, V. R. *Cell. Mol. Life Sci.* **2002**, *59*, 1833−1850.
(5) Viviani, V. R.; Arnoldi, F. G.; Neto, A. J.; Oehlmeyer, T. L.; Bechara, E. J.; Ohmiya, Y. *Photochem. Photobiol. Sci.* **2008**, *7*, 159−169.
(6) Fraga, H. *Photochem. Photobiol. Sci.* **2008**, *7*, 145−158.
(7) Hosseinkhani, S. *Cell. Mol. Life Sci.* **2011**, *68*, 1167−1182.
(8) Navizet, I.; Liu, Y. J.; Ferré, N.; Roca-Sanjuán, D.; Lindh, R. *ChemPhysChem* **2011**, *12*, 3064−3076.
(9) Hasegawa, J. Y.; Fujimoto, K. J.; Nakatsuji, H. *ChemPhysChem* **2011**, *12*, 3106−3115.
(10) Naumov, P.; Ozawa, Y.; Ohkubo, K.; Fukuzumi, S. *J. Am. Chem. Soc.* **2009**, *131*, 11590−11605.
(11) Naumov, P.; Kochynnoonny, M. *J. Am. Chem. Soc.* **2010**, *132*, 11566−11579.
(12) Pinto da Silva, L.; Esteves da Silva, J. C. G. *ChemPhysChem* **2011**, *12*, 951−960.
(13) Hirano, T.; Hasumi, Y.; Ohtsuka, K.; Maki, S.; Niwa, H.; Yamaji, M.; Hashizume, D. *J. Am. Chem. Soc.* **2009**, *131*, 2385−2396.
(14) Chen, S. F.; Liu, Y. J.; Navizet, I.; Ferré, N.; Fang, W. H.; Lindh, R. *J. Chem. Theory Comput.* **2011**, *7*, 798−803.
(15) Song, C.; Rhee, Y. M. *J. Am. Chem. Soc.* **2011**, *133*, 12040−12049.
(16) Pinto da Silva, L.; Esteves da Silva, J. C. G. *J. Comput. Chem.* **2011**, *32*, 2654−2663.
(17) Pinto da Silva, L.; Esteves da Silva, J. C. G. *ChemPhysChem* **2011**, *12*, 3002−3008.
(18) Pinto da Silva, L.; Esteves da Silva, J. C. G. *J. Phys. Chem. B* **2012**, *116*, 2008−2013.
(19) Tagami, A.; Ishibashi, N.; Kato, D.; Taguchi, N.; Mochizuki, Y.; Watanabe, H.; Ito, M.; Tanaka, S. *Chem. Phys. Lett.* **2009**, *472*, 118−123.
(20) Milne, B. F.; Marques, M. A.; Nogueira, F. *Phys. Chem. Chem. Phys.* **2010**, *12*, 14285−14293.
(21) Nakatani, N.; Hasegawa, J. Y.; Nakatsuji, H. *J. Am. Chem. Soc.* **2007**, *129*, 8756−8765.
(22) Esteves da Silva, J. C. G.; Magalhães, J. M. C. S.; Fontes, R. *Tetrahedron Lett.* **2001**, *42*, 8173−8176.
(23) Erez, Y.; Huppert, D. *J. Phys. Chem. A* **2010**, *114*, 8075−8082.
(24) Presiado, I.; Erez, Y.; Huppert, D. *J. Phys. Chem. A* **2010**, *114*, 9471−9479.
(25) Presiado, I.; Erez, Y.; Huppert, D. *J. Phys. Chem. A* **2010**, *114*, 13337−13346.
(26) Erez, Y.; Presiado, I.; Gepshtein, R.; Huppert, D. *J. Phys. Chem. A* **2011**, *115*, 1617−1626.
(27) Presiado, I.; Gepshtein, R.; Erez, Y.; Huppert, D. *J. Phys. Chem. A* **2011**, *115*, 7591−7601.
(28) Morton, R. A.; Hopkins, T. A.; Seliger, H. H. *Biochemistry* **1969**, *8*, 1598−1607.
(29) Jung, J.; Chin, C. A.; Song, P. S. *J. Am. Chem. Soc.* **1976**, *98*, 3949−3954.
(30) Ando, Y.; Akiyama, H. *Jpn. J. Appl. Phys.* **2010**, *49*, 117002−117006.
(31) Ribeiro, C.; Esteves da Silva, J. C. G. *Photochem. Photobiol. Sci.* **2008**, *7*, 1085−1090.
(32) Ireland, J. E.; Wyatt, P. A. *Adv. Phys. Org. Chem.* **1976**, *12*, 131−221.
(33) (a) Gutman, M.; Nachliel, E. *Biochem. Biophys. Acta* **1990**, *1015*, 391−414. (b) Pines, E.; Huppert, D. *J. Phys. Chem.* **1983**, *87*, 4471−4478.
(34) Tolbert, L. M.; Solntsev, K. M. *Acc. Chem. Res.* **2002**, *35*, 19−27.
(35) Rini, M.; Magnes, B. Z.; Pines, E.; Nibbering, E.T. J. *Science* **2003**, *301*, 349−352.
(36) Mohammed, O. F.; Pines, D.; Dreyer, J.; Pines, E.; Nibbering, E. T. J. *Science* **2005**, *310*, 83−86.
(37) Tran-Thi, T. H.; Gustavsson, T.; Prayer, C.; Pommeret, S.; Hynes, J. T. *Chem. Phys. Lett.* **2000**, *329*, 421−430.
(38) Agmon, N. J. *Phys. Chem. A* **2005**, *109*, 13−35.
(39) Spry, D. B.; Fayer, M. D. *J. Chem. Phys.* **2008**, *128* (084508), 1−9.
(40) Siwick, B. J.; Cox, M. J.; Bakker, H. J. *J. Phys. Chem B* **2008**, *112*, 378−389.
(41) Mohammed, O. F.; Pines, D.; Nibbering, E. T. J.; Pines, E. *Agnew. Chem. Intern. Ed.* **2007**, *46*, 1458−1461.
(42) Mondal, S. K.; Sahu, K.; Sen, P.; Roy, D.; Ghosh, S.; Bhattacharyya, K. *Chem. Phys. Lett.* **2005**, *412*, 228−234.
(43) Prasun, M. K.; Samanta, A. *J. Phys. Chem. A* **2003**, *107*, 6334−6339.
(44) Bhattacharya, B.; Samanta, A. *J. Phys. Chem. B* **2008**, *112*, 10101−10106.